

In-Flight Center-of-Gravity Estimation Using Extended Kalman Filter

Khadeeja Nusrath TK, Basappa, Jatinder Singh
Scientists, Flight Mechanics & Control Division
CSIR-NAL, Bangalore, India.

G Kumar Babu
ITIVIT, Mumbai, India

Abstract—Inaccuracy in the center of gravity position can adversely affect the aerodynamic estimation results. A technique is proposed wherein, using flight path reconstruction in EKF framework, the aircraft cg is estimated from flight measurements alone, without using any additional information on the fuel consumed or aircraft mass or inertias. The accuracy of the estimated center of gravity is verified using coefficient level matching and time response matching from closed loop aircraft simulation model.

Keywords—Center-of-gravity, EKF, acceleration, flight path reconstruction

I. INTRODUCTION

One of the challenges in aircraft stability and control analysis is the accurate estimation of center of gravity (CG). This issue has mostly been addressed by solving the weight and balance problem using fuel burn data. However, the inaccuracies present in the fuel burn calculations lead to erroneous computation of CG.

For flight maneuvers with partially filled fuel tanks, the center of gravity varies due to fuel sloshing and continuous fuel consumption. The randomness in the CG position causes changes to the control surface deflections especially during pitch maneuvers. Lateral offset in CG gives rise to unwanted rolling effects.

In flight mechanics studies, accurate information about aircraft mass, inertia and CG location is essential for aerodynamic modeling and estimation of stability and control parameters. The accuracy of center of gravity position is crucial in the process of aerodynamic database validation and update from flight test data using system identification techniques.

Some attempts have been made in the past to calculate the aircraft CG position. In 1998, Blakely and Hedges [1] developed the method of separating aircraft into nodes and calculating CG of each node by introducing fuel slosh time lag that was computed from aircraft pitch rate. An alternate method was presented in a patent by Sundstrand Corporation (Glover, 1985) based on setting two sets of accelerometer sensors at near and farther end of the aircraft. Accelerations from each set of sensors were computed around CG and equated to compute the CG location [2]. Andrew J. Komendat and Agamemnon L. Crassidis in their research paper used standard aircraft measurements to estimate CG [3]. A longitudinal CG estimator using state estimation technique

was developed by Andrew Stanley and Roger Goodall in Ref. [9]. Online computation of CG of a flight vehicle from kinematics is described in Ref. [11].

In this paper, the work reported in Ref. [3] and [9] is extended to estimate the CG of a fly by wire high performance fighter aircraft from flight data. To maintain proper weight distribution, the aircraft was equipped with a fuel proportioner to deliver fuel to the engine in such a manner that the deviation in CG was minimal [4]. Further, to account for the changes in CG and inertia due to the change in aircraft mass resulting from fuel depletion during high angles-of-attack maneuvers, mass and balance calculations were repeated taking into consideration the fuel pitch angle settings. The fuel pitch angle for this purpose was calculated using the measured longitudinal and vertical accelerations [4].

A novel method is discussed for estimating the aircraft center of gravity using only the flight data measurements. In this approach, CG estimation is implemented as part of normal flight path reconstruction procedure, in which Extended Kalman Filtering (EKF) technique is used for joint state and parameter estimation [5]. The proposed algorithm uses an optimization approach to translate the accelerometer data measured at a known sensor location on the body to a location where nominal expected conditions about the center-of-gravity during flight test are observed. The algorithm presented is based purely on the aircraft flight dynamics and does not use any of the fuel or mass and inertia information, which is the biggest advantage of the model. Moreover, there is no necessity of extra sensors to be installed in the aircraft to carry out CG estimation.

II. METHODOLOGY OF CG ESTIMATION

An aircraft engine conventionally receives fuel supply from fuel tanks located in the wings and fuselage. Placement of large fuselage tanks distributed fore and aft along the fuselage is a common feature on high speed aircraft because of the difficulty in finding sufficient fuel capacity within thin wings and also because of the desire for high-fineness ratio of fuselage [5]. Fuel sloshing not only affects the fuel measurement but also the CG and moments-of-inertia. Theoretical studies show that location of the oscillating fuel mass ahead of the airplane's CG has a strong destabilizing effect on the airplane's short-period motion [6]. Dependent on CG location are also the lever arms of various sensors such as accelerometers and airflow sensors.

When the aircraft is in rotatory motion, acceleration on the body changes from one point to another. The measured accelerations at the sensor location need to be translated from sensor to center of gravity by applying the force equations given in (4). This translation from sensor to CG requires accurate information of the center of gravity location.

A. Relative motion in rigid body

$$\mathbf{v} = \boldsymbol{\omega} \times \mathbf{r} \quad (1)$$

As the body axes rotates about the center of gravity with angular velocity $\boldsymbol{\omega}$ w.r.t inertial axes. The relative velocity between two points (A, B) in the body axes can be written as

$$\mathbf{v}_{B/A} = \boldsymbol{\omega} \times \mathbf{r}_{B/A} \quad (2)$$

$$\mathbf{v}_B = \mathbf{v}_A + \boldsymbol{\omega} \times \mathbf{r}_{B/A}$$

Equations (1) and (2) hold only when there is no relative motion between the points A and B in the rotating frame, which is satisfied through aircraft rigid body assumption. Differentiating Eq.(2), acceleration relation between the two points in rotating rigid body can be known

$$\mathbf{a}_B = \mathbf{a}_A - \boldsymbol{\alpha} \times \mathbf{r}_{B/A} + \boldsymbol{\omega} \times (\boldsymbol{\omega} \times \mathbf{r}_{B/A}) \quad (3)$$

$$\boldsymbol{\alpha} = \dot{\boldsymbol{\omega}}$$

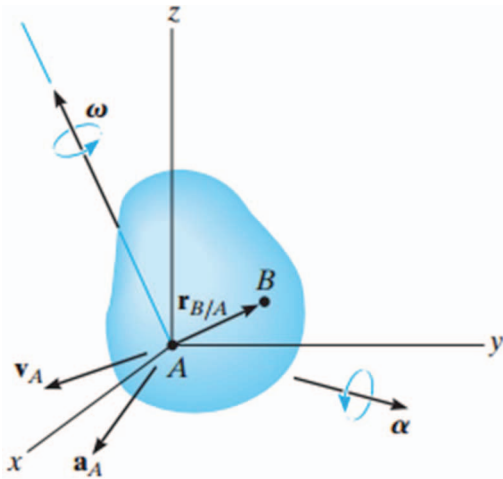


Fig. 1. Instantaneous rigid body rotation

Since the accelerometers mounted away from the CG measure local accelerations which contain the components due to the angular rates and accelerations, it is necessary to obtain the linear accelerations at CG. From (3), the acceleration can be calculated at any point provided the acceleration at some other point and its displacement from that point is known [7].

The rotational velocity of the body $\boldsymbol{\omega}$ is observed through the angular rates p, q, r . Substituting the above parameters in (3), acceleration can be translated from sensor to CG location using measurable quantities as follows.

$$\begin{aligned} a_x &= a_{xs} + (q^2 + r^2) x_{ascg} - (pq - \dot{r}) y_{ascg} - (pr - \dot{q}) z_{ascg} \\ a_y &= a_{ys} - (pq - \dot{r}) x_{ascg} + (p^2 + r^2) y_{ascg} - (qr - \dot{p}) z_{ascg} \\ a_z &= a_{zs} - (pr - \dot{q}) x_{ascg} - (qr + \dot{p}) y_{ascg} + (p^2 + q^2) z_{ascg} \end{aligned} \quad (4)$$

Where (p, q, r) are the measured angular rates, and $\dot{p}, \dot{q}, \dot{r}$ the angular accelerations obtained by numerical differentiation of the measured angular rates. X_{ascg}, Y_{ascg} and Z_{ascg} denote the position of the accelerometer sensors with respect to the CG along the three body-fixed coordinate axes, respectively [8].

In an aircraft, a three-axis accelerometer measures accelerations in all the three directions and its position with respect to reference datum should be known. Table 1 describes the sensor offset corrections for the 3 accelerometers.

TABLE1: Sensor offset

ax, ay, az accelerometer sensor arms in body fixed frame					
from Datum			from CG		
X	Y	Z	X	Y	Z
x_{as}	y_{as}	z_{as}	x_{ascg}	y_{ascg}	z_{ascg}
Where, $x_{ascg} = -(x_{as} - x_{cg})$; $y_{ascg} = y_{as} - y_{cg}$; $z_{ascg} = -(z_{as} - z_{cg})$ x_{cg} +ve forward, y_{cg} +ve right and z_{cg} +ve down					

Implementing the information from Table 1 into (4), CG location x_{cg}, y_{cg}, z_{cg} can be estimated as augmented states in the flight path reconstruction using Extended Kalman Filter. This CG estimation methodology is represented in Fig. 2.

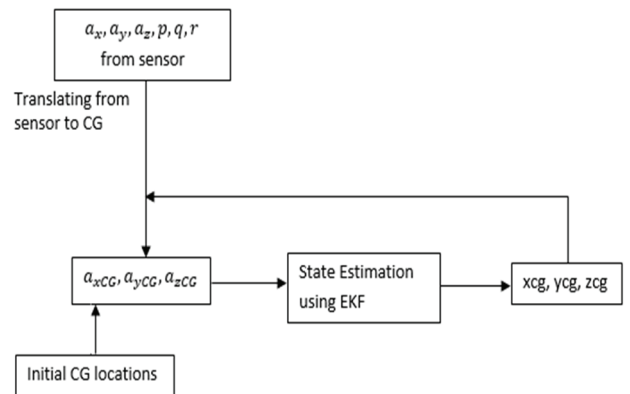


Fig. 2. CG Estimation Methodology Block diagram

B. Flight Path Reconstruction

Flight path reconstruction (FPR) primarily deals with the estimation of aircraft states and determination of instrument errors such as biases, scale factors and time delays in the measurements. The results (data signals) obtained from this phase are expected to be 'bias free'. In the current investigations, FPR is carried out with 7 states and 6 observations. The inertial velocities in the body axis (u, v, w) , the Euler angles (ϕ, θ, ψ) and altitude h are the estimated states. The observed variables from flight data used in FPR analysis are the angle of attack α_m , true air speed V_m , pressure altitude h_m and Euler angles ϕ_m, θ_m, ψ_m . The state and observation models for FPR are discussed next[5].

State equations:

$$\begin{aligned}\dot{u} &= -(q - \Delta q)w + (r - \Delta r)v - g \sin \theta + (a_x - \Delta a_x) + w_u \\ \dot{v} &= -(r - \Delta r)u + (p - \Delta p)w + g \cos \theta \sin \phi + (a_y - \Delta a_y) + w_v \\ \dot{w} &= -(p - \Delta p)v + (q - \Delta q)u + g \cos \theta \cos \phi + (a_z - \Delta a_z) + w_w \\ \dot{\phi} &= (p - \Delta p) + (q - \Delta q) \sin \phi \tan \theta + (r - \Delta r) \cos \phi \tan \theta + w_\phi \\ \dot{\theta} &= (q - \Delta q) \cos \phi - (r - \Delta r) \sin \phi + w_\theta \\ \dot{\psi} &= (q - \Delta q) \sin \phi \sec \theta + (r - \Delta r) \cos \phi \sec \theta + w_\psi \\ \dot{h} &= u \sin \theta - v \cos \theta \sin \phi - w \cos \theta \cos \phi + w_h\end{aligned}\quad (5)$$

Where $\Delta a_x, \Delta a_y, \Delta a_z, \Delta p, \Delta q, \Delta r$ are the biases in rates and accelerations. The process noise is defined as

$$[w_u \ w_v \ w_w \ w_\phi \ w_\theta \ w_\psi \ w_h]^T$$

To start with, initial values of the state variables are taken as the average of the first few values from the measurements and then iterated upon to get the correct estimates.

$$\begin{aligned}u(0) &= u_0, v(0) = v_0, w(0) = w_0, \phi(0) = \phi_0, \theta(0) = \theta_0, \\ \psi(0) &= \psi_0, h(0) = h_0\end{aligned}\quad (6)$$

The accelerations converted from sensor to CG in (4) are substituted in state model given in (5).

Since the aircraft velocities in the body frame relative to wind cannot be measured directly, it requires the knowledge of wind profile. The wind components are also estimated as augmented states. Thus, the body velocities of the aircraft relative to wind are computed by

$$[u_c \ v_c \ w_c]^T = [uvw]^T - [w_x \ w_y \ w_z]^T\quad (7)$$

w_x, w_y, w_z are the wind velocities in body axes.

The flow angles and true airspeed can be obtained from the estimated states using the following relations:

$$\begin{aligned}\alpha &= \tan^{-1}(w_c / u_c) \\ \beta &= \sin^{-1}(v_c / V) \\ V &= \sqrt{(u_c)^2 + (v_c)^2 + (w_c)^2}\end{aligned}$$

Observation equations:

$$\begin{aligned}V_m &= V + v_v \\ \alpha_m &= (K_\alpha \alpha + \Delta \alpha) + v_\alpha \\ \beta_m &= (K_\beta \beta + \Delta \beta) + v_\beta \\ \phi_m &= \phi + v_\phi \\ \theta_m &= \theta + v_\theta \\ \psi_m &= \psi + v_\psi \\ h_m &= h + v_h\end{aligned}\quad (8)$$

Equation. (8) considers a simple sensor model for α and β , where K_α and K_β are the calibration scale factors and $\Delta \alpha$ and $\Delta \beta$ are the unknown bias errors. The measurement noise is given by

$$[v_v, v_\alpha, v_\beta, v_\phi, v_\theta, v_\psi, v_h]^T$$

The state input and observation vector for the FPR can be defined as

$$x = [u \ v \ w \ \phi \ \theta \ \psi \ h]^T$$

$$u = [a_x \ a_y \ a_z \ p \ q \ r]^T$$

$$y = [V \ \alpha \ \beta \ \phi \ \theta \ \psi \ h]^T\quad (9)$$

From the above state and observation equations, the unknown parameter vector to be estimated is given by

$$\begin{aligned}\Theta &= [x_{cg} \ y_{cg} \ z_{cg} \ \Delta a_x \ \Delta a_y \ \Delta a_z \ \Delta p \ \Delta q \\ \Delta r \ K_\alpha \ \Delta \alpha \ K_\beta \ \Delta \beta \ w_x \ w_y \ w_z]^T\end{aligned}\quad (10)$$

III. ESTIMATION METHOD

In this paper, state estimation is performed by using Extended Kalman Filtering (EKF). This nonlinear technique helps to estimate the states accurately in the presence of process and measurement noise. Using EKF, the parameter estimation problem is transformed into state estimation problem by defining an augmented state vector as

$$x_a = [x^T \Theta^T]^T \quad (11)$$

Here the estimated parameter vector Θ augmented to the state vector x , where the subscript ‘‘a’’ denotes the augmented variables. Thus, for FPR using EKF, the state and observation models can be expressed as

$$\begin{aligned} \dot{x}_a(t) &= f[x_a(t), u(t)] + w(t) \\ y(t) &= g[x_a(t), u(t)] \\ z(t_k) &= y(t_k) + v(t_k) \end{aligned} \quad (12)$$

where $w(t)$ and $v(t_k)$ are the state and measurement noise vector, $z(t_k)$ is the vector of observations at the k^{th} time instant. Equation (5) can be substituted into (12) to estimate the augmented state vector.

The model in (12) assumes Gaussian white noise with zero mean. A priori specification of the covariance matrices of the measurement and process noise is necessary to use EKF [8]. The measurement noise covariance matrix is obtained from the characteristics of the instrumentation used in the aircraft. Since process noise is considered as the noise in the input signals, the variances of the accelerometer and rate gyro measurement noise are used to define the process noise covariance matrix [8,10].

IV. VALIDATION OF ESTIMATED CG

The accuracy of estimated CG has an effect on the moment coefficient computed at reference point from flight measured signals and also on the time trajectory simulations. A fidelity check on the estimated CG is carried out by using coefficient level matching and through time response matching of 6DOF simulation trajectories with flight measured signals.

A. Coefficient level matching with estimated CG

Coefficient level matching is the process of comparing the total aerodynamic force and moment coefficients that are computed from flight data with those derived from reference aerodynamic database (ADS). The corresponding difference between two sets (ΔC_i) is delta (Δ) model as given in the (13).

$$\Delta C_i = C_{i_{\text{Flight}}} - C_{i_{\text{ADS}}} \quad (13)$$

The flight derived moment coefficients calculated at CG are then transferred to moment reference point about which the aerodynamic model is developed. Computation of flight derived moment coefficients will be erroneous if incorrect CG location is used for transferring from CG to moment reference point. The identified error ΔC_i also will be incorrect. Equation (14) gives conversion of pitching moment coefficient C_m from CG to moment reference.

$$C_m^{AC} = C_m^{CG} - C_x \frac{Z_{ACCG}}{cbar} + C_z \frac{X_{ACCG}}{cbar} \quad (14)$$

Where C_x and C_z are the force coefficients and (X_{ACCG} , Z_{ACCG}) the position of the moment reference point with respect to CG. $cbar$ is the mean aerodynamic chord.

B. Time Response matching with estimated CG

The flight identified increments or ‘‘ Δs ’’ from the coefficient error models are added to the baseline aerodynamic database as shown in (13) and closed-loop simulation in time domain is carried out for validation of the updated database [4].

For the time response matching with estimated CG, pilot commands are fed into the closed loop simulation model with aero-database and control laws. The simulated time responses so obtained are compared with the actual flight measured responses. To verify the correctness of CG estimate, the trajectories were simulated for the CG from weight and balance table look up and compared with those obtained with estimated CG.

V. RESULTS & DISCUSSION

A. CG Estimation

The flight maneuver data gathered at high angles of attack is used for proving the concept of CG estimation. Fig. 3 gives the flight trajectory match during flight path reconstruction using EKF along with the error plots for V , α and β . The close match ensures the correctness of the CG estimate, which is estimated as an augmented state from the FPR. The autocorrelation of the residuals satisfies the whiteness test and the values are well within the 95 per cent confidence limits.

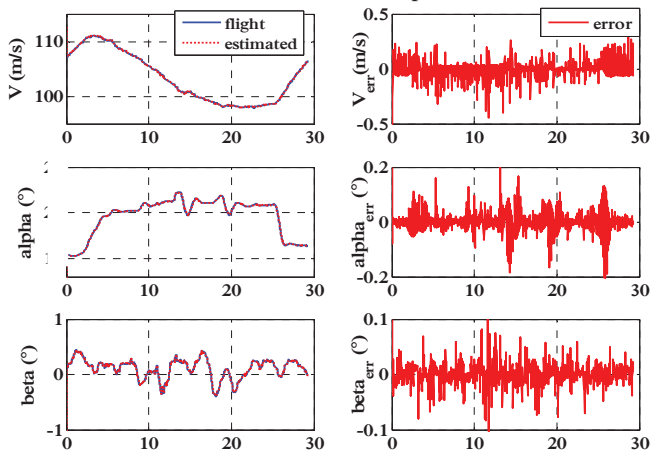


Fig. 3. Estimated and Measured states and the corresponding error

The accelerometer biases and CG positions can be correlated during estimation when both are estimated together. The delta changes in accelerations due to change of CG is shown in Fig.4 and the peak difference is observed to be of the order 10^{-4} which is much less than order of bias in acceleration measurements. So inaccurate biases estimate in the calculations may result in erroneous CG locations estimates. Initially, biases for accelerations are estimated for a level flight, where CG effects are negligible and CG estimation carried out for maneuvering regime with the known Δx , Δy , Δz values fixed. Table-2 list the bias values estimated for linear accelerations and rates from a level flight data along with error bounds (standard deviations). The scale factor in angle of attack and side slip is found to be unity and bias is zero, since the air data tables are already updated using flight test procedures.

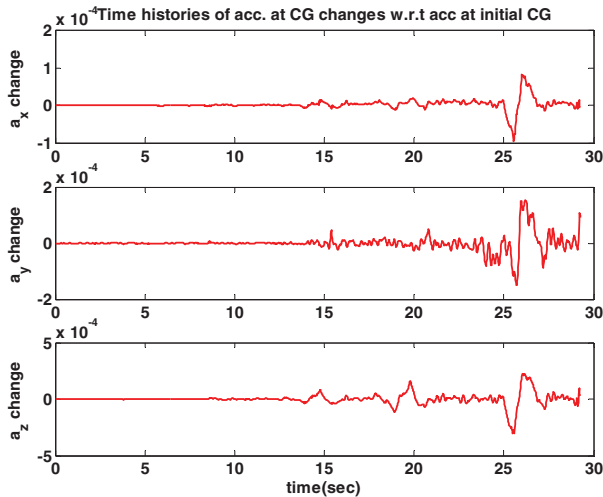


Fig. 4. Time history of change in acceleration w.r.t change initial CG location.

TABLE-2 Estimated biases in linear accelerations

Parameter	Estimated value	Standard deviation
Δx (m/s)	4.01191e-02	5.8837e-03
Δy (m/s)	2.36025e-02	2.9336e-02
Δz (m/s)	-3.31195e-02	2.4068e-02
Δp (rad/s)	4.10642E-03	1.6432e-06
Δq (rad/s)	-1.05494E-04	5.6527e-07
Δr (rad/s)	-9.22516E-04	3.2694e-06

The initial values for the covariance corresponding to the state variables $P(x)$, $\text{diag}(0.01I_{7 \times 7})$ and augmented states $P(\theta)$, $\text{diag}(0.001I_{16 \times 16})$. The diagonals of Q and R are defined either from information provided by instrumentation specifications or from the data noise characteristics. To help the convergence of the estimates, R is set $\text{diag}(0.005, 1 \times 10^{-5}I_{2 \times 2}, 1 \times 10^{-6}I_{3 \times 3}, 0.2)$ and $Q(x) = \text{diag}(0.00005, 0.009, 0.002, 1 \times 10^{-10}I_{3 \times 3}, 0.2)$ for states, $Q(\theta) = \text{diag}(0I_{6 \times 6}, 0.5I_{3 \times 3})$ for augmented states.

Fig. 5 shows the estimated CG compared with the CG obtained from mass-CG (weight and balance calculations) lookup tables accounting for the effects due to fuel pitch angle. Y axis values are normalized in Fig. 5.

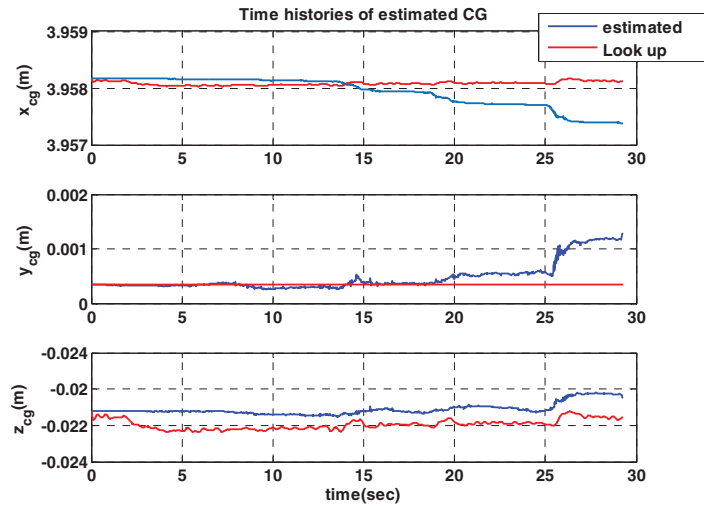


Fig. 5. Comparison of CG estimate with CG from look-up tables

B. CG Validation

Effect of CG correction on pitching moment coefficient is shown in Fig. 6, where the delta error in pitching moment coefficient (ΔC_m vs α) for the CG from look-up tables is compared with the ΔC_m computed for the estimated CG. The error in C_m is observed to be less with the estimated CG.

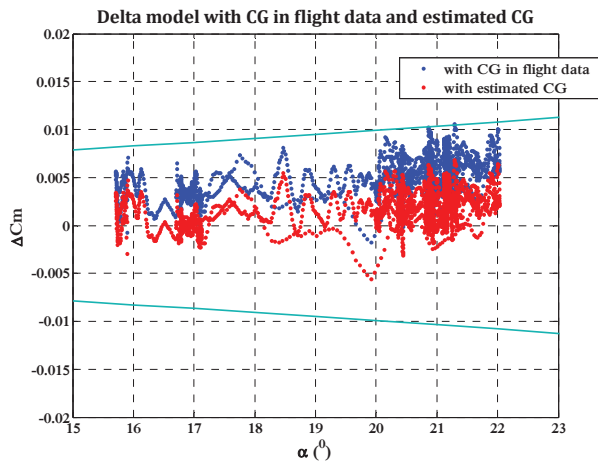


Fig. 6. comparison of Error in C_m with use of estimated CG location & from look up table.

Fig. 7 compares the flight recorded elevator input with the one obtained from close loop simulation, with and without CG correction. It is evident from the figure that with estimated CG, the simulated δ_e is in better agreement with the flight δ_e .

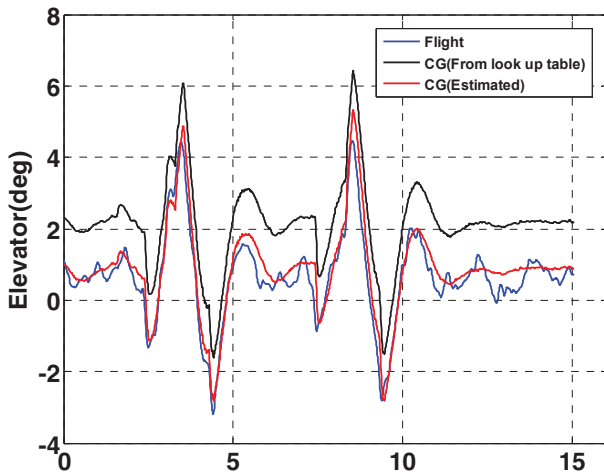


Fig.7. Comparison of flight and simulated elevator deflection using different CG locations

VI. CONCLUSIONS

A novel approach for estimating center of gravity from aircraft flight data is discussed. The center of gravity is estimated as

an augmented state in EKF state estimator. Noise covariance matrices in EKF are manually tuned and their robustness verified over several data segments. Coefficient level matching and closed loop time response matching are used to verify the accuracy of estimated CG position. Corrected CG position further leads to the use of correct values of mass and inertias resulting in better accuracy in the stability and control estimation.

Acknowledgment

The authors wish to thank Aeronautical Development Agency for providing support for this research work.

References

- [1] Blakely, P., and Hedges, D. (1998) "A real-time application for computing gross weight and center of gravity measurements on Boeing experimental test flights" Proceedings of International Symposium, Instrumentation in the Aerospace Industry, pp. 211-218.
- [2] Glover, J. (1985), Patent No. 4545019. USA
- [3] Andrew J. Komendat and Agamemnon L. Crassidis, "Center of gravity estimation using standard aircraft measurement sensors", AIAA Atmospheric Flight Mechanics Conference 13-16 August 2012, Minneapolis, Minnesota (2012).
- [4] Kaliyari, D., Nusrath TK, K., and Singh, J. (2015). "Validation and update of aerodynamic database at extreme flight regimes", SAE Technical Paper 2015-01-2567, DOI: 10.4271/2015-01-2567.
- [5] Nusrath, K., Sarmah, A., and Singh, J., "Flight path reconstruction and wind estimation using flight test data from crash data recorder (CDR)," SAE Technical Paper 2014-01-2168, 2014, doi:10.4271/2014-01-2168.
- [6] Perkins Courtland D., "Flight test manual, stability and control, Volume II," AGARD, 1959
- [7] R. C. Hibbeler, Engineering Mechanics: Statics and Dynamics.
- [8] Jategaonkar, R.V. (2006), Flight Vehicle System Identification - A Time Domain Methodology, AIAA Progress in Astronautics and Aeronautics, Vol. 216, AIAA, Reston, VA
- [9] Stanley, A. and Goodall, R. (2009) "Estimation of aircraft center of gravity using kalman filters", Proc. of European Control Conference, Aug 23-26 2009, pp 1848-1853.
- [10] G. Welch & G. Bishop, An introduction to the Kalman filter, Retrieved October 21st, 2008, from University of North Carolina :http://www.cs.unc.edu/~welch/media/pdf/kalman_intro.pdf
- [11] Tahk M J, Trikas T and Wallace B "Post flight Data Reduction Techniques for Hovered Kinetic Energy Weapons", Journal of Guidance, Control and Dynamics, pp. 872-877, Vol. 17, No 4, September-October (1991).